Pyranoanthocyanins: A Theoretical Investigation on Their Antioxidant Activity

Monica Leopoldini, Francesca Rondinelli, Nino Russo,* and
Marirosa Toscano

*Dipartimento di Chimica and Centro di Calcolo ad Alte Prestazioni per
Elaborazioni Parallele e Distribuite-Centro d'Eccellenza MIUR, Università della Calabria,
I-87030 Arcavacata di Rende (CS), Italy*

The antioxidant radical scavenging capacity of pyranoanthocyanins present in aged wine and coming from the chemical transformation undergone by anthocyanins was theoretically explored by DFT/B3LYP methods. The two main working mechanisms (H atom donation and single-electron transfer) were investigated, and the O−H bond dissociation energy (BDE) and ionization potential (IP) parameters were computed in the gas phase and in water and benzene solutions. Results indicated that systems possessing the catechol functionality as well as the *o*-dimethoxy motif are good candidates to donate a H atom to the free radicals, inactivating them. Compounds with a higher degree of electron delocalization may work within the single-electron transfer mechanism. Results provided molecular insight into factors that influence the radical scavenging potential of anthocyanins and then the beneficial health effects of these wine pigments.

INTRODUCTION

Phenolic compounds are plant secondary metabolites commonly found in herbs and fruits such as berries, apples, citrus fruit, grapes, vegetables such as onions, olives, tomatoes, broccoli, lettuce, and soybeans, grains and cereals, green and black tea, coffee beans, propolis, and red and white wines (*1*−*9*).

In recent decades, they have attracted growing global interest upon the discovery of the so-called "French paradox", that is, the observation that although many French use tobacco products and have a diet rich in fats, they show much reduced rates of coronary heart diseases when compared with northern European nations such as the United Kingdom and Germany (*10*). The most popular explanation for these findings is recognized in the relatively high daily consumption by the French of red wine rich in phenolic compounds, which in some way act to protect them from heart diseases (*11, 12*).

All phenolic compounds possess a common structural feature: an aromatic ring bearing at least one hydroxyl substituent. A further classification divides them in simple phenols and polyphenols (*13,14*), possessing at least two phenol subunits, and including the flavonoids, the stilbenes, and those compounds having three or more phenol subunits (hydrolyzable and nonhydrolyzable tannins) (*14*). The basic structural feature of flavonoids is the flavan (2-phenyl-benzo-γ-pyran) nucleus, a system of two benzene rings (A and B) linked by an oxygen-containing pyran ring (C) (see **Scheme 1**).

Anthocyanins belong to the flavonoids group and are responsible for the red and blue colors of plant organs such as fruits, flowers, and leaves (*15*).

Anthocyanins are believed to act as antioxidants (*16*), but they have also been proposed to have other biological activities that produce beneficial effects on health (*17*−*20*).

Anthocyanins are responsible for the color of red wine as they are extracted from grape berries during the winemaking process. Wine is a product that undergoes many different changes during aging in wood and storage in bottles. One of the altered parameters during aging is the color, which is a very important sensory characteristic of red wine (*21*). The important role played by anthocyanins in determining the color of red wine is well-known. In fact, anthocyanins are converted, through chemical transformations during wine aging, to new pigments that become responsible for the changing color and the longevity of wine (*22*).

The new pigments formed were first thought to result mainly from condensation reactions between anthocyanins and flavanols directly or mediated by acetaldehyde (*23*−*29*). Nevertheless, over the past decade, reactions involving anthocyanins with other compounds such as pyruvic acid (*30*−*35*), vinylphenol (*36, 37*), vinylcatechol (*38*), α-ketoglutaric acid (*39*), acetone (*39*−*41*), and 4-vinylguaiacol (*41*) have been demonstrated to yield new families of anthocyanin-derived pigments, namely, pyranoanthocyanins, with spectroscopic features that may somehow contribute to a more orange-red color.

The molecular basis for the antioxidant properties of polyphenols and thus of anthocyanins is revealed in three main mechanisms, arising from the reaction with free radicals (*42*−*45*) and from the chelation of metals (*46*). As primary antioxidants, polyphenols inactivate free radicals according to hydrogen atom transfer (1) and single-electron transfer (2)

*Author to whom correspondence should be addressed (e-mail nrusso@unical.it).

Published on Web 07/13/2010

Article

J. Agric. Food Chem., Vol. 58, No. 15, 2010   **8863**

Scheme 1. Structures of Pyranoanthocyanins
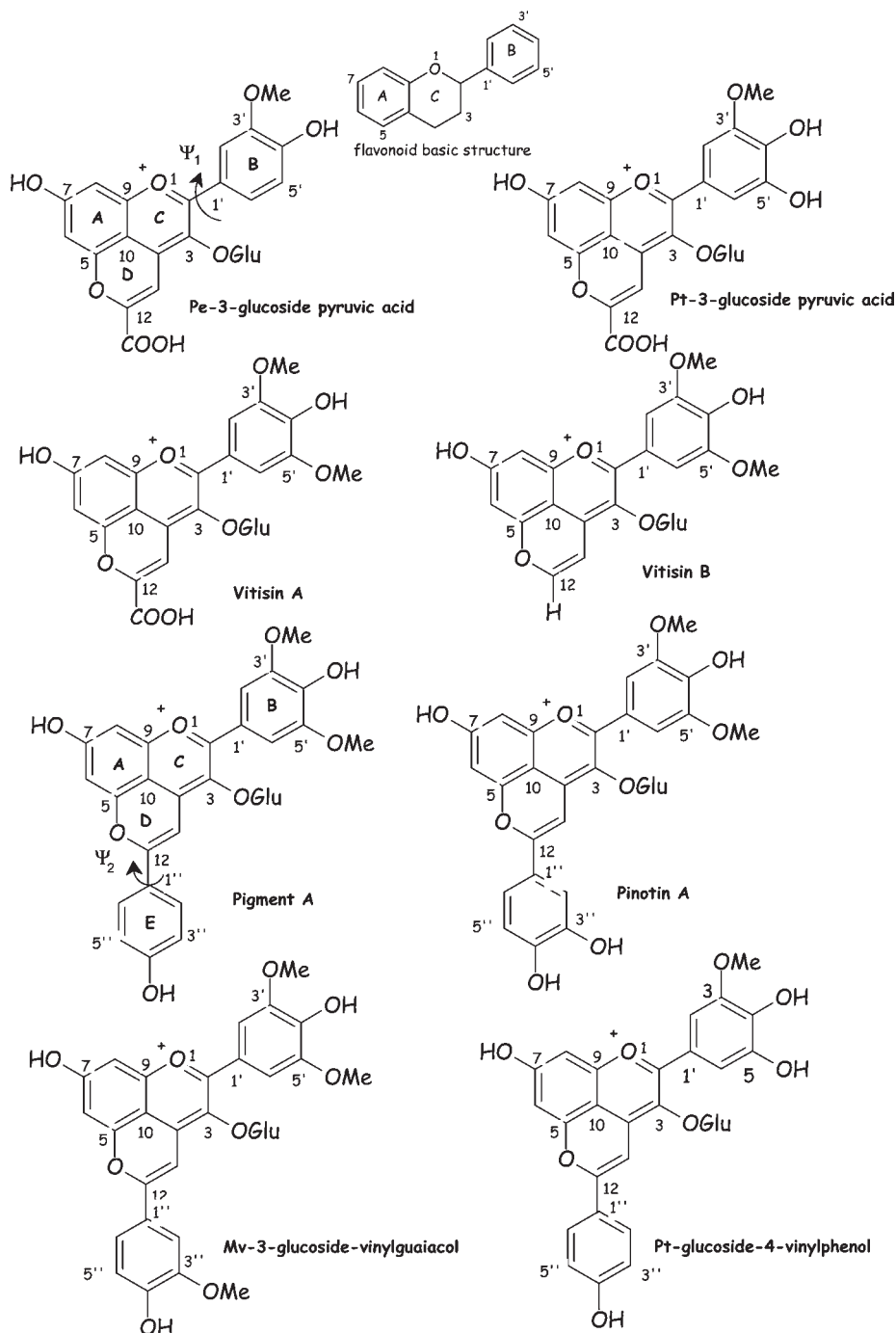
mechanisms. In mechanism 1, the antioxidant (ArOH) reacts with the free radical (R$^{\bullet}$) by transferring to it a hydrogen atom.

$$ArOH + R^{\bullet} \rightarrow ArO^{\bullet} + RH \qquad (1)$$
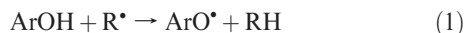
The products of the reaction are the harmless RH species and the oxidized ArO$^{\bullet}$ radical. ArO$^{\bullet}$ is much less reactive regarding R$^{\bullet}$ because it is usually stabilized by several factors (*42*–*46*).

The single-electron transfer mechanism 2 provides an electron to be donated to the R$^{\bullet}$:

$$ArOH + R^{\bullet} \rightarrow ArOH^{\bullet+} + R^{-} \qquad (2)$$
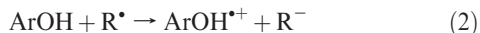
The anion R^{-} is an energetically stable species with an even number of electrons, whereas the cation radical ArOH$^{\bullet+}$ is also in this case a less reactive radical species.

The mechanism of chelation of transition metal cations such as iron (*46*), lead (*47*), aluminum (*48*), and copper (*49*) has shown that flavonoids may represent good chelating agents.

Most of flavonoids are believed to act through the H atom transfer because higher energies are involved in the one-electron transfer process (*42*).

In the past decade, many computational studies have been devoted to the elucidation of phenolics' and flavonoids' antioxidant activity. Particularly, several DFT investigations concerning the determination of the bond dissociation energy (BDE) of phenolic OH groups and the ionization potential (IP) (*42*–*45*) have given considerable information about the antioxidant ability because the lower the BDE and IP values are, the more favored are the hydrogen abstraction and the electron-transfer reactions. The gas-phase values of BDE and IP computed for flavonoids

usually fall in the ranges of 70−90 and 160−190 kcal/mol, respectively.

At the present, to the best of our knowledge, the antioxidant capability of pyranoanthocyanins has not been investigated computationally, so that an important gap in the comprehension of red wine chemistry and biochemistry as well as of the health-promoting effects of wine consumption still exists.

The main aim of this study is to determine the geometrical and electronic features of eight pyranoanthocyanins from aged wine. Furthermore, to corroborate the antioxidant capability of these compounds within the working mechanisms proposed in the literature, the BDE and IP thermodynamic parameters have been computed as the more representative descriptors for the radical scavenging ability of flavonoids.

MATERIALS AND METHODS

All geometries of anthocyanin-derived pigments and of their radicals were optimized without constraints, using tight convergence criteria, employing the DFT/B3LYP (UB3LYP for the resulting radicals) exchange-correlation functional and the 6-311+G* basis set, as implemented in the Gaussian03 computational programs suite (*50*). The inclusion of polarization functions correctly takes into account intramolecular H bonding.

Vibrational frequencies were obtained at the same level of theory, at 298 K and 1 atm, with the aim to characterize all structures as minima and to estimate zero-point energy corrections that were included into the electronic energies.

Single-point energy calculations using the 6-311++G** basis set were performed at B3LYP level on the 6-311+G* optimized geometries and used to refine electronic energies. This basis set of triple-ζ quality, including polarization and diffuse functions, was extensively used for studying antioxidant polyphenolic compounds and had provided very reliable results (*43−46*).

The unrestricted open-shell approach was used for radical species. No spin contamination was found for radicals; values were 0.750 in all cases.

Solvent effects were computed within the framework of self-consistent reaction field polarizable continuum model (SCRF-PCM), implemented in the Gaussian program (*50*), using the UA0 set of solvation radii to build the cavity for the solute, in the gas-phase equilibrium geometries. This model was used for both the parent molecules and their respective radicals. This is a simple representation for treating long-range solvent effects and considers the solvent as a macroscopic continuum with a dielectric constant and the solute as filling a cavity in this continuous medium. The dielectric constants of 78.39 and of 2.25 were chosen to reproduce the water and benzene media, respectively.

Natural bond orbital (NBO) analysis was used to characterize the electronic structures of the systems under investigation.

The OH BDE and IP values were computed at 298 K as the sum of the enthalpy of the radical resulting from the hydrogen atom abstraction and that of the hydrogen atom minus the enthalpy of the parent molecule and as the enthalpy difference between the radical cation and the parent molecule, respectively.

RESULTS

Pyranoanthocyanin Minima Structures. The pyranoanthocyanin structures studied here are presented in **Scheme 1**. They are peonidin-3-glucoside-pyruvic acid (Pe-3-GluPA), petunidin-3-glucoside-pyruvic acid (Pt-3-GluPA), vitisin A, vitisin B, pigment A, pinotin A, malvidin-3-glucoside-vinylguaiacol (Mv-3-GluVG), and petunidin-3-glucoside-4-vinylphenol (Pt-3-GluVP). To reduce the computational effort due to the large size of these compounds, the glucoside moiety has been replaced by a methyl group. Additionally, it is very unlikely that the sugar ring may have some influence on the reactivity of the systems, because the reactive site is universally accepted to be the flavonoid part (*42*), which has been kept unchanged in our model system.

B3LYP geometry minimization of Pe-3-GluPA, Pt-3-GluPA, vitisin A, and vitisin B compounds (see Figure S1 in the Supporting Information) finds as minima the conformations exhibiting an intense π electron delocalization and conjugation that involve rings A, C, and D. For pigment A, pinotin A, Mv-3-GluVG, and Pt-3-GluVP (Figure S1 in the Supporting Information), also ring E is involved in this phenomenon. Ring B seems not to be implicated in the whole electron π delocalization, as the $C_3-C_2-C_{1'}-C_{2'}$ dihedral (Ψ_1) values for Pe-3-GluPA (163.6°), Pt-3-GluPA (162.3°), vitisin A (163.5°), vitisin B (162.6°), pigment A (159.7°), pinotin A (160.2°), Mv-3-GluVG (160.6°), and Pt-3-GluVP (159.7°) indicate. Therefore, all calculations result in nonplanar structures for pyranoanthocyanins.

Minimum energy conformers are all arranged so as to maximize the number of intramolecular H bonds, especially at the B ring. In fact, in all molecules, the 4'OH donates a H bond to the adjacent 3'OCH$_3$ group, whereas a further H bond with the 5'OH group is established in the case of Pt-3-GluPA (2.23 Å) and Pt-3-GluVP (2.22 Å) molecules. Pinotin A and Mv-3-GluVG present another H bond in ring E, established between the 3''OH and 4''OH groups (2.18 Å) and between the 3''OCH$_3$ and 4''OH groups (2.11 Å).

Previous theoretical works on anthocyanidin aglycones have offered contradictory results to the question of whether or not they adopt planar conformation in their minimum energy structure. A theoretical analysis of anthocyanidins performed using the DFT-B3LYP/6-31G(d) approach (*51*) has found that these compounds are nonplanar, with the 2-phenyl ring twisted relative to the benzopyrylium rings by 7.52° (flavylium), −4.98° (apigeninidin), 2.19° (cyanidin), 3.75° (delphinidin), 2.21° (luteolinidin), −7.91° (malvidin), 1.82° (pelargonidin), −10.70° (peonidin), and −28.14° (petunidin). Vinylpyranoanthocyanin−phenolic pigments (portisins), structures that are very similar to the subject of this study, have been predicted to assume a nonplanar disposition in the minima employing the B3LYP/6-31G(d) protocol, and the conformations have been determined by the flexibility of the sugar moiety and by the interaction of the latter (steric hindrance and hydrogen bonds) with the B ring (*52*). Rings B and AC have pointed to coplanarity for flavylium cations in a study performed at AM1 and DFT levels, in both the gas and aqueous phases, even if a reasonable number of twisted quinonoidal bases have been found in both phases (*53*). Cyanidin has converged to a planar conformation in a B3LYP/6-311++G** study (*44*). DFT/B3LYP/D95 investigations about molecular structures and excited states of pelargonidin, cyanidin, delphinidin, and aurantinidin (*54*) have pointed out that planar structures are slightly more stable than the nonplanar ones, the two conformations being dictated by the orientation of the 3OH group belonging to the C ring. Aurantinidin, cyanidin, delphinidin, malvidin, pelargonidin, and peonidin global minima have been found to be planar at the B3LYP/6-31G(d,p) level (*55*). Finally, B3LYP/6-311++G** conformational analysis of delphinidin, pelargonidin, cyanidin, peonidin, petunidin, and malvinidin cationic species has indicated a planar conformation in all examined cases (*56*).

With regard to the results presented in this study, the deviation from planarity, regarding B and ACD rings (Ψ_1), can be viewed as a balance between conjugation, which favors planar structures, and steric hindrance, due to the presence of the −OCH$_3$ group (that replaces the bulky sugar ring) at the C3 position. Furthermore, the presence of rings D and E may draw electron flow, enhancing the possibility of delocalization and conjugation in this part of the molecule.

Therefore, the torsional potential between the phenyl B ring and the 1,4-benzopyrone skeleton in anthocyanins and generally

Article

J. Agric. Food Chem., Vol. 58, No. 15, 2010   **8865**

Table 1. Pyranoanthocyanin Radical Relative Energies (Kilocalories per Mole)

compound	radical					
	3′OH	4′OH	5′OH	7OH	3″OH	4″OH
Pe-3-glucoside pyruvic acid		0.0		5.9		
Pt-3-glucoside pyruvic acid		0.0	6.4	12.2		
vitisin A		0.0		8.9		
vitisin B		0.0		9.9		
pigment A		0.0		9.0		7.3
pinotin A	1.7			10.7	1.0	0.0
Mv-3-glucoside vinylguaiacol		0.0		9.5		3.9
Pt-3-glucoside 4-vinylphenol		0.0	6.2	11.2		9.5

in flavonoids has been found to be almost flat within ±30° of the planar geometry with very low barrier heights that are in some cases below the accuracy of the employed methodology.

To analyze the torsion around the C2—C1′ bond, a fully relaxed torsional potential is computed for Pe-3-Glu-PA at the B3LYP level of theory in vacuo. The potential energy curve is obtained as a function of the dihedral angle around the C2—C1′ bond by scanning it in steps of 10°, starting from the 163.6° value. Results are reported in Figure S2 in the Supporting Information. All conformers fall in a range of 0−9.47 kcal/mol. A relative minimum is found at 0.16 kcal/mol for a dihedral value of −16.4°. Two maximum energy conformers of Pe-3-Glu-PA are found at 8.84 and 9.47 kcal/mol for dihedral values of −96.4° and 83.6°, respectively.

Radicals from Hydrogen Abstraction. By abstracting a hydrogen atom from every hydroxyl group present on the pyranoanthocyanin molecules, two (Pe-3-GluPA, vitisins A and B), three (Pt-3-GluPA, pigment A, and Mv-3-GluVG), and four (pinotin A and Pt-3-GluVP) radical species are obtained. The relative energies of all radicals are presented in **Table 1**. The optimized geometries of all radicals are available in the Supporting Information. **Figure 1** shows the spin density distribution of the most stable radicals of anthocyanin pigments.

The Pe-3-Glu-PA 4′OH radical, arising from the abstraction of a hydrogen atom from the OH group attached at the 4′ carbon, is more stable than the 7OH by 5.9 kcal/mol (see Figure S3 in the Supporting Information). This difference in energy can be explained by considering that in the 4′OH radical species, apart from the possibility of resonance effects, the electronic vacancy generated on the radical formation center is stabilized by hyperconjugation with the adjacent methyl group occurring through a simple rotation of 180° around the $C_{3'}$−O bond. The 4′OH radical isomer lacking this kind of interaction is energetically less stable by 1.8 kcal/mol. Plotting of the 4′OH radical spin density distribution (**Figure 1**) shows how the odd electron remains on the radical oxygen atom, with a lesser involvement of the adjacent methoxy group. The stability of the 7OH radical arises only from the possibility of resonance effects between rings A and C.

H atom abstraction in Pt-3-GluPA pigment leads to the formation of three radicals, among which the most stable is again the 4′OH (see Figure S4 in the Supporting Information). The 5′OH and 7OH species lie at 6.4 and 12.2 kcal/mol, respectively, above the absolute minimum. The electron deficiency originated at the 4′OH site is supplied not only by the hyperconjugation with the $C_{3'}$−OCH$_3$ group but also by the H bond with the $C_{5'}$OH that is retained in going from parent molecule to radical. The spin distribution observed in **Figure 1** exhibits the involvement of the whole ring B in the delocalization of the unpaired electron. Pt-3-GluPA radical 5′OH has as principal stabilization source the intramolecular H bond established with the $C_{4'}$OH group. This kind of interaction is absent in the 7OH species, so its relative energy is higher.

Radical formation from the vitisin A molecule gives rise to two radicals, 4′OH and 7OH, the latter found at 8.9 kcal/mol above the former, which is the absolute minimum. By looking at the optimized geometries described in Figure S5 in the Supporting Information, one can realize the positive effect arising from the hyperconjugation of the two adjacent −CH$_3$ groups occurring only in the 4′OH species. Unpaired spin density is mainly found in the radical 4′O (**Figure 1**).

Upon the H atom abstraction process, vitisin B also generates two radicals, 4′OH and 7OH (see Figure S6 in the Supporting Information), the latter found at 9.9 kcal/mol above the 4′OH representing the absolute minimum. The arguments developed to explain the energy differences between conformers of vitisin A radicals can be repeated in this case. However, an element that must be emphasized now is that the absence of the −COOH substituent in ring D entails a lesser stabilization of the 7OH radical of 1.0 kcal/mol (see the relative energies of vitisin A and B 7OH radicals reported in **Table 1**).

7OH and 4″OH radicals of pigment A are found at 9.0 and 7.3 kcal/mol above the 4′OH absolute minimum (see Figure S7 in the Supporting Information). Here, the hyperconjugation effects predominate over the possibility of delocalization of the unpaired electron, because radical formation at ring E does not produce the most stable radical species.

The radical formation process in pinotin A yields four radical species, of which the 4″OH is the absolute minimum. The other species are found at 1.0 (3″OH), 1.7 (4′OH), and 10.7 (7OH) kcal/mol (see Figure S8 in the Supporting Information). The 4″OH species presents the stabilizing effect of the catechol moiety due to the establishment of an intramolecular H bond (2.10 Å). Atomic spin density reported in **Figure 1** shows that the unpaired electron is located mostly on the C1″ and C5″ in ring E and partially also on the C13 carbon in ring D, proving that a certain delocalization of the odd electron is effective between these two rings. The 3″OH radical feels the stabilizing effects from the intramolecular hydrogen bond so that it is almost isoenergetic with the 4″OH species. In the 3″OH radical, a deviation from the planar conformation occurs. In fact, the Ψ_2 dihedral between rings E and D changes from 176.1° in the parent pinotin A to 161.6° in the 3″OH radical, whereas for the others it is 176.9° (4′OH), 179.1° (7OH), and 174.7° (4″OH).

Mv-3-GluVG radical formation entails the formation of three radicals: 4′OH (0.0 kcal/mol), 7OH (9.5 kcal/mol), and 4″OH (3.9 kcal/mol) (see Figure S9 in the Supporting Information). The absolute minimum is the 4′OH radical, from which the relative energy value is mainly determined by the hyperconjugation of two CH$_3$ groups on the electronic vacancy site. Spin density distribution (**Figure 1**) involves the whole molecule except ring E. In the 4″OH radical, only one methyl is involved in the hyperconjugation phenomenon, so that its slightly higher value of energy (3.9 kcal/mol) can be considered as a measure of the stabilizing effect of the additional methyl group. Again, for the 7OH radical, the possibility of stabilization of the unpaired electron is confined to resonance phenomena.

Finally, radicals arising from H atom abstraction from the Pt-3-GluVP molecule are 4′OH, 5′OH, 7OH, and 4″OH (reported in Figure S10 in the Supporting Information), from which relative energies are 0.0, 6.2, 11.2, and 9.5 kcal/mol, respectively. In the 4′OH species, both the methyl hyperconjugation and the intramolecular H bond concur to the stabilization of the unpaired electron. As can be noted in **Figure 1**, the unpaired electron spin density is found predominantly at the phenolic O• atom and at the methoxy group in ring C. 5′OH is stabilized by the intramolecular H bond established with the vicinal 4′OH hydroxyl group. 7OH and 4″OH stabilization is set up by the possibility of several
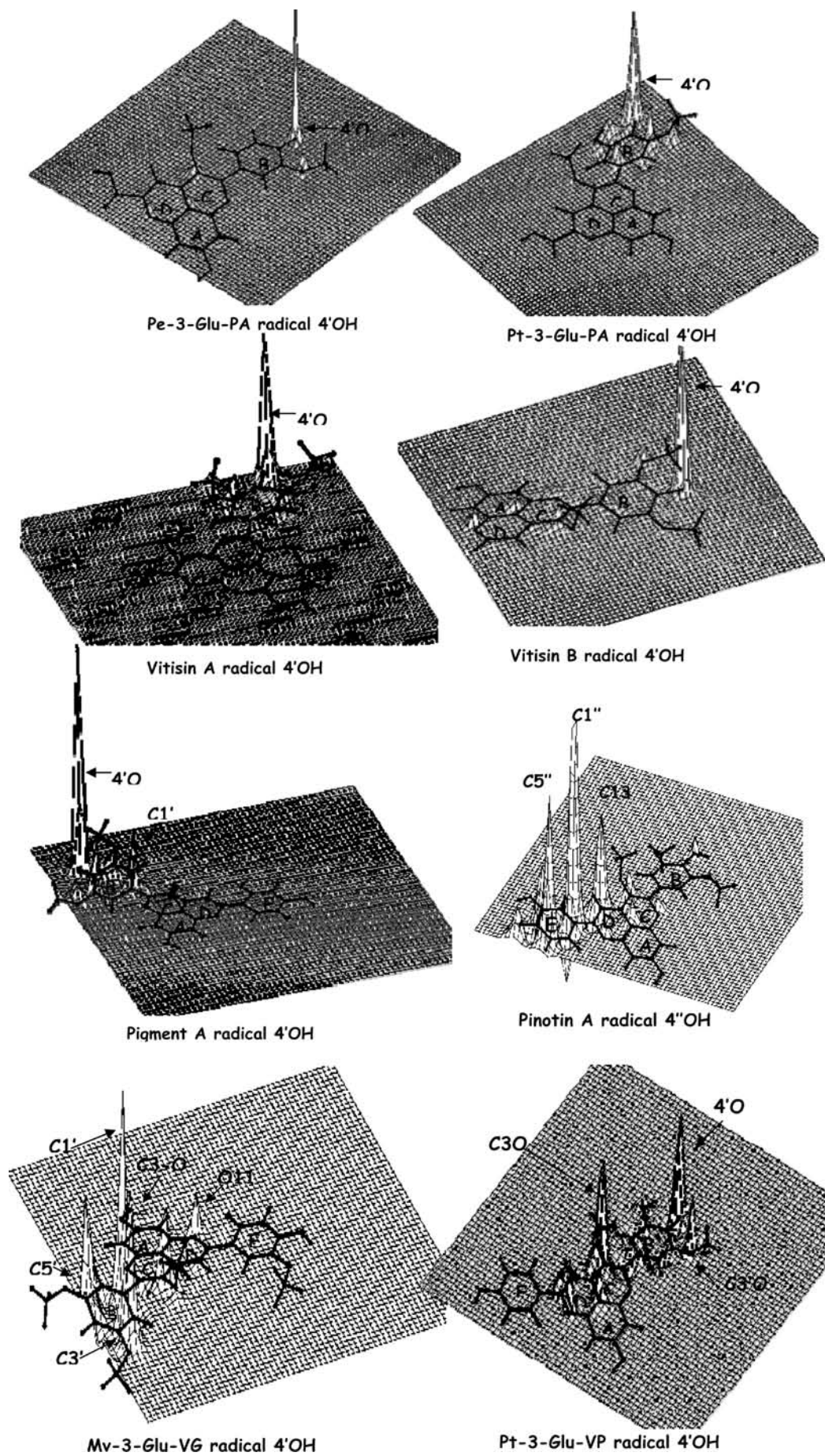
Figure 1. Plotting of the spin density distribution of pyranoanthocyanins' most stable radicals.

resonance structures, but this phenomenon better occurs when radical formation takes place at ring E rather than at ring A, as confirmed by the relative energies of the 4″OH and 7OH (9.5 and 11.2 kcal/mol, respectively) radicals.

The most reliable site that may lose a hydrogen atom in pyranoanthocyanins is the 4′OH group in ring B. This occurs because the radicals originated by this process are species in which the electronic vacancy is compensated by the hyperconjugation involving the overlap with the neighboring C−H σ bond orbital, the intramolecular H bond formation with adjacent OH groups, and the delocalization of the odd electron. The only exception is represented by pinotin A molecule in which radical formation preferentially occurs at the 4″OH group in ring E, because the intramolecular H bond between the O• and the adjacent −OH energetically predominates over the hyperconjugation between O• and the adjacent −OCH$_3$ groups.

Spin density in radicals is mainly found on the phenolic O atom from which the hydrogen is abstracted. As far as the radical formation in Mv-3-GluVG and Pt-3-GluVP is concerned, the spin distribution of the unpaired electron is not confined on the O• but involves also atoms belonging to rings C and D, despite the nonplanar conformation (as far as Ψ$_1$ is concerned) adopted by parent molecules and radicals. However, even if anthocyanins adopt nonplanar arrangements in their minimum energy geometries, they may exist in different conformations depending on the small oscillation of the phenyl ring B with regard to rings A−C, in which energy differences are not so significant (*56*). Therefore, during radical formation, anthocyanin may form a planar structure with a very low energy cost in order to reach the better distribution of the unpaired electron.

Radicals from Electron Abstraction. As reported in the Introduction, antioxidants may also act according to the one-electron transfer mechanism, in which a radical cation ArOH•+ arises. The optimized geometries of the radical cations are reported in the Supporting Information. **Figure 2** shows the spin density distribution for these radicals.

Radical cation from Pe-3-Glu-PA is a nonplanar species (Ψ$_1$ = 163.7°) as in the parent molecule, retaining also the H bond at the catechol moiety (2.16 Å). Spin density is mainly found at ring B, and in particular it involves the methoxyl and hydroxyl groups and also the C1′ carbon atom. The methoxyl group replacing the sugar moiety in ring C is affected by spin density to a lesser degree (see **Figure 2**).

For Pt-3-Glu-PA radical cation, spin density involves the oxygen atoms in ring B and, to a larger degree, the C3 position in ring C (**Figure 2**), despite the nonplanar arrangement between rings B and AC (Ψ$_1$ = 162.9°). The H bond pattern in ring B is retained in going from parent molecule to the radical cation.

Vitisin A radical cation shows a spin density distribution involving mainly rings B and C, as reported in **Figure 2**, whereas for vitisin B spin density is confined to ring B, even if they exhibit similar C3−C2−C1′−C2′ dihedrals (158.4 and 159.6°). The −COOH group in vitisin A, replaced by a hydrogen atom in vitisin B, draws the unpaired electron density.

In pigment A radical cation, spin density distribution involves almost the whole molecule except ring A, as can be noted from **Figure 2**. Geometry optimization converges to a nonplanar structure with a Ψ$_1$ = 161.7° and a planarity between rings E and D (Ψ$_2$ = 178.8°).

The electron abstraction process from pinotin A generates a radical cation in which the odd electron is mainly found at ring B, particularly at the C4′OH moiety.

The Mv-3-Glu-VG radical cation shows a great spin density that involves the whole molecule except ring A, whereas the Pt-3-Glu-VP radical formation process through electron abstraction produces a radical in which the unpaired electron density is confined to ring B and partially to ring C.

When a single electron is abstracted from the HOMO of pyranoanthocyanin molecules to form radical cations, the unpaired electron is spread in different ways depending on the phenolic substitution. In the case of Pe-3-Glu-PA, vitisin B, pinotin A, and Pt-3-Glu-VP, the unpaired electron density is found on ring B, whereas it is shared as much as possible in the whole molecules of Pt-3-Glu-PA, vitisin A, pigment A, and Mv-3-Glu-VG compounds.

DISCUSSION

The OH BDEs computed for all anthocyanin pigments are collected in **Table 2**. Values, in the gas and condensed phases (water and benzene), refer to the most stable 4′OH radical species, except for pinotin A, for which 4″OH represents the minimum energy conformer. As can be noted, BDE gas-phase values are included in the range of 78.2−85.5 kcal/mol. Corrections in solution cause an increase of these values by around 10 kcal/mol, in both the water and benzene media.

The compound showing the lowest value of BDE is Pt-3-Glu-VP, both in vacuo (78.2 kcal/mol) and in the condensed phase (88.4 and 87.4 kcal/mol, in water and benzene, respectively), followed by pinotin A, the BDE values of which are 78.5, 89.9, and 88.8 kcal/mol, in vacuo, in water and in benzene, respectively. Both systems possess the *o*-dihydroxy functionality, at rings B and E, respectively. The high electron delocalization involving the aromatic rings quite affects the value of BDE. The additional methoxy group at 3′-position in ring B in Pt-3-Glu-VP contributes to further decrease the BDE.

Pt-3-Glu-PA shows BDEs of 79.2, 89.4, and 88.6 kcal/mol in the gas phase, water, and benzene, respectively. The difference in gas-phase BDEs of 1.0 kcal/mol between Pt-3-Glu-VP and Pt-3-Glu-PA underscores the positive effect associated with the presence of ring E, which is lacking in Pt-3-Glu-PA.

When no dihydroxy functionality occurs, the possibility of hyperconjugation between methyl groups and radical oxygen influences the BDE values. This effect is higher when two methyl groups are present in the ortho position with respect to the OH, as confirmed by the BDE values for Pe-3-Glu-PA of 85.5 and 94.4 kcal/mol, in vacuo and in water and benzene media.

These findings confirm the key role played by the dihydroxy functionality that causes a stabilization of radicals originated upon H atom abstraction, so that a lowest value of BDE is obtained. Also, the presence of two methoxy groups adjacent to the OH that undergoes the radical formation process is another important structural parameter that entails low BDE values. Also, ring E, enhancing the possibility of conjugation and delocalization, determines low BDEs.

B3LYP/6-31G(d,p) BDE values for the 4′OH group in anthocyanins have been computed to be 86.8 kcal/mol for cyanidin, 96.0 kcal/mol for malvidin, and 95.8 kcal/mol for peonidin (*56*). Computations at the B3LYP/6-31G(d)// 6-311G(2d,2p) level have yielded gas-phase BDE values of 87.0, 80.2, 80.4, and 88.9 kcal/mol, for cyanidin-3-*β*-*O*-glucoside, delphinidin (3′,4′,5′,3,5,7-hexahydroxy), delphinidin-3-*O*-*β*-glucoside, and malvidin-3-*O*-*β*-glucoside, respectively, as far as the 4′OH hydroxyl is concerned (*57*). 4′OH BDE in delphinidin has been computed to be 75.5 kcal/mol in both gas phase and water solution at the B3LYP/6-31++G(d,p) level (*58*).

Upon comparison with the available literature data, it is worth noting that the presence of rings D and E in pyranoanthocyanins
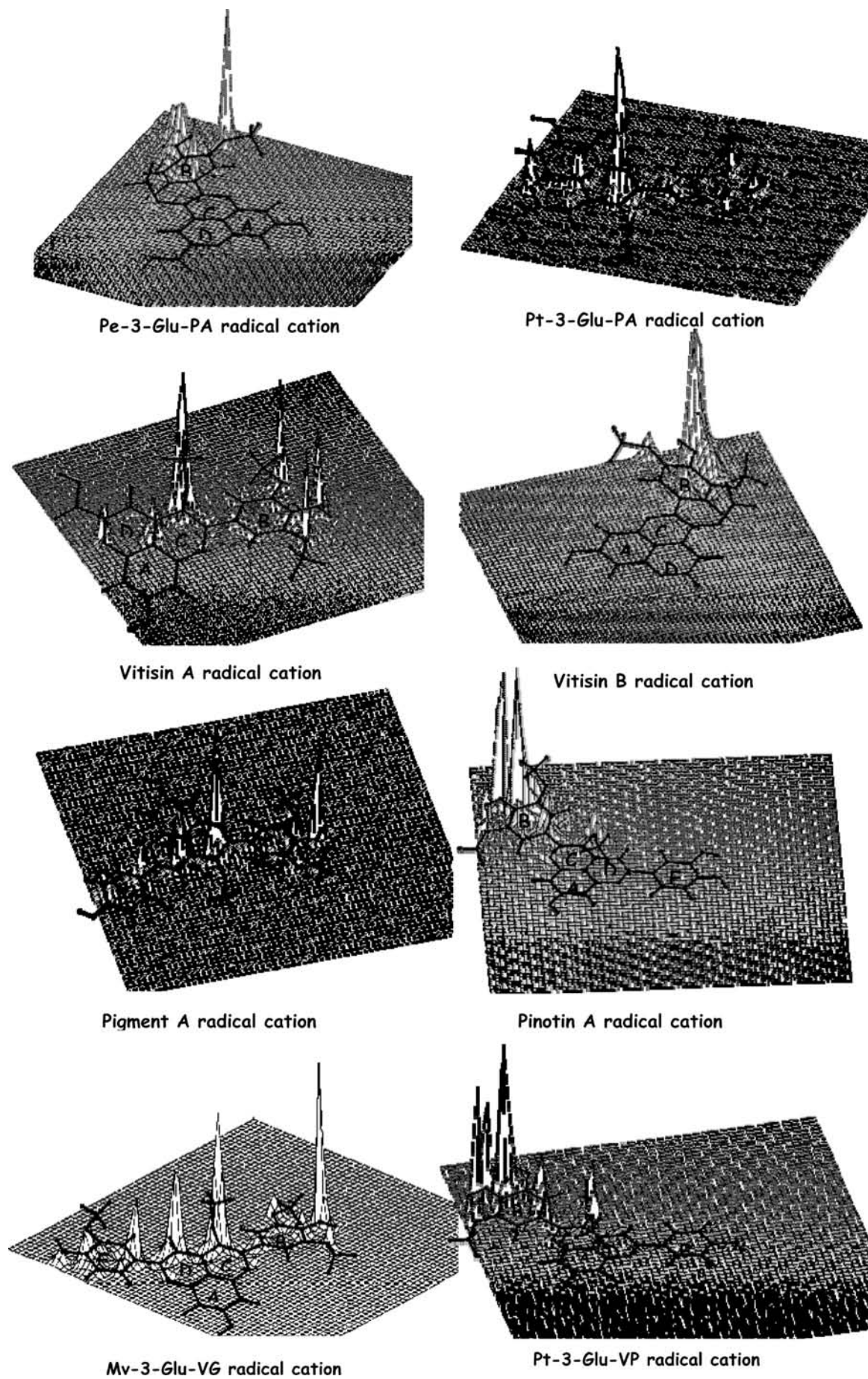
Pe-3-Glu-PA radical cation

Pt-3-Glu-PA radical cation

Vitisin A radical cation

Vitisin B radical cation

Pigment A radical cation

Pinotin A radical cation

Mv-3-Glu-VG radical cation

Pt-3-Glu-VP radical cation

Figure 2. Plotting of the spin density distribution of pyranoanthocyanins' radical cations.

Table 2. Bond Dissociation Energies (BDE) in the Gas Phase and in Water and Benzene Media

	BDE (kcal/mol)		
compound	gas phase	water	benzene
Pe-3-glucoside pyruvic acid	85.5	94.3	94.3
Pt-3-glucoside pyruvic acid	79.2	89.4	88.6
vitisin A	81.7	94.2	92.2
vitisin B	80.8	91.7	90.8
pigment A	80.2	91.1	90.1
pinotin A	78.5	89.9	88.8
Mv-3-glucoside vinylguaiacol	79.7	90.8	89.8
Pt-3-glucoside 4-vinylphenol	78.2	88.4	87.4

Table 3. Ionization Potentials (IP) in the Gas Phase and in Water and Benzene Media

	IP (kcal/mol)		
compound	gas phase	water	benzene
Pe-3-glucoside pyruvic acid	237.3	140.0	184.0
Pt-3-glucoside pyruvic acid	236.0	138.8	183.2
vitisin A	230.1	137.7	179.8
vitisin B	230.5	138.0	179.4
pigment A	220.1	136.5	174.1
pinotin A	219.4	136.4	175.6
Mv-3-glucoside vinylguaiacol	217.8	136.2	173.4
Pt-3-glucoside 4-vinylphenol	223.2	135.6	175.3

contributes to the lowering of the energy required for breaking the O−H bond (BDE) regarding anthocyanins, thus making easier the hydrogen atom donation. Therefore, Pe-3-Glu-PA is a better radical scavenger with respect to peonidin anthocyanin, because BDE for the 4′OH decreases by around 10 kcal/mol. Also, Mv-3-Glu-VG, with a BDE value of 79.7 kcal/mol, exhibits a larger antioxidant capability than malvidin anthocyanidin (*55*) (BDE = 96.0 kcal/mol) and its glucoside derivative (BDE = 88.9 kcal/mol) (*57*).

In **Table 3**, the IP values in the gas phase, and in water and benzene solutions are reported for all pyranoanthocyanins. One has to remember that electron donation by positively charged pyranoanthocyanins determines the formation of a cation with a +2 charge, so that gas-phase IP values are larger as compared to uncharged flavonoid IPs reported in the literature. Solvation lowers decidedly the energy required to extract a single electron, in both the water and benzene solutions.

The compound exhibiting the lowest value of gas-phase IP is Mv-3-GluVG (217.8 kcal/mol), followed by pinotin A, pigment A, and Pt-3-Glu-VP (219.4, 220.1, and 223.2 kcal/mol, respectively). These compounds possess the further ring E that seems to contribute to the lowering of the IP values, probably determining a better distribution of the unpaired electron. Vitisins A and B, Pt-3-Glu-PA, and Pe-3-Glu-PA, lacking this moiety, present higher values of IP (see **Table 3**).

Water solution lowers the values of computed IP by electrostatic interactions with the double-charged radicals. Furthermore, the solvent reduces the range of IPs so that all values are included between 140.0 and 135.6 kcal/mol. The better pyranoanthocyanin in donating a single electron within the water solution is Pt-3-Glu-VP (IP = 135.6 kcal/mol).

Also, benzene medium lowers the IPs (to a lesser degree relative to the water) with respect to the gas phase. Pyranoanthocyanins, despite their positive charge, are quite soluble in benzene, probably due to the aromatic rings present in the molecule. Pt-3-Glu-VP shows again the lowest value of IP, whereas

Pe-3-Glu-PA possesses the highest one (175.3 and 184.0 kcal/mol, respectively).

Unfortunately, only a few theoretical investigations about ionization potentials in anthocyanin compounds are available in the literature. Delphinidin IP has been computed to be 240.7 kcal/mol in the gas phase and 133.3 kcal/mol in the aqueous solution at the B3LYP/6-31++G(d,p) level (*44*). Gas-phase IP for cyanidin has been computed to be 246.2 kcal/mol (*44*).

Theoretical results show that in the case of the mechanism of the electron transfer, the main factors affecting the value of IP are the extended delocalization and conjugation of the π-electrons, enhanced by resonance phenomena, rather than the presence of a particular functional group such as additional hydroxyls, also according to literature results concerning flavonoids (*44*).

In conclusion, we have applied a density functional based method employing the B3LYP functional to the study of naturally occurring antioxidant compounds. Particularly, we have focused on pyranoanthocyanins deriving from the chemical transformations undergone by anthocyanins during wine aging, which are responsible for the color, feel, and taste as well as longevity of aged wines.

The main mechanisms proposed in the literature for the antioxidant action of polyphenols as radical scavengers, consisting of the H atom and electron transfer, have been discussed in detail, and structural and electronic features of radical species arising from these mechanisms have been determined.

The OH BDE and the adiabatic IP have been computed, both in the gas phase and in solutions, because they represent excellent primary indicators of the radical scavenging activity exhibited by these compounds.

On the basis of our investigation, we can outline the following conclusions:

Pyranoanthocyanins are not completely planar systems because in all cases ring B is twisted with respect to the rest of the molecule by around 20°. However, conjugation and delocalization of the π electrons occur in pyranoanthocyanins and involve the aromatic ring(s) and the substituents.

Upon removal of a hydrogen atom or an electron within the H atom or the electron-transfer process, respectively, pyranoanthocyanins give rise to radical species in which the odd electron appears to be delocalized as much as possible over the whole molecule.

As far as the H atom transfer mechanism is concerned, the stability of radicals is enhanced by the possibility that they establish intramolecular H bonds between the radical oxygen atom and vicinal hydroxyl. When the catechol functionality is absent, the hyperconjugation phenomena with vicinal OCH_3 and the presence of an additional aromatic ring become important for the radical's stability.

BDE values are within a range of 78.2−85.5 kcal/mol in the gas phase, whereas solutions show an increase in the values of around 10 kcal/mol. They are, anyway, smaller with respect to the BDE value of the phenol compound usually taken as reference.

Within the one-electron transfer mechanism, good candidates are those compounds that show wide electron delocalization.

8870 *J. Agric. Food Chem.,* Vol. 58, No. 15, 2010

Leopoldini et al.

Supporting Information Available: Figures S1−S10. This material is available free of charge via the Internet at http://pubs.acs.org.

LITERATURE CITED

(1) Ross, J. A.; Kasum, C. M. Dietary flavonoids: bioavailability, metabolic effects, and safety. *Annu. Rev. Nutr* 2002, *22*, 19–34.

(2) Hertog, M. G. L.; Hollman, P. C. H.; Katan, M. B.; Kromhout, D. Intake of potentially anticarcinogenic flavonoids and their determinants in adults in the Netherlands. *Nutr. Cancer* 1993, *20*, 21–29.

(3) Brit, D. F.; Hendrich, S.; Wang, W. Dietary agents in cancer prevention: flavonoids and isoflavonoids. *Pharmacol. Ther.* 2001, *90*, 157–177.

(4) Kris-Etherton, P. M.; Hecker, K. D.; Bonanome, A. B.; Coval, S. M.; Binkoski, A. E.; Hilpert, K. F.; Griel, A. E.; Etherton, T. D. Bioactive compounds in foods: their role in the prevention of cardiovascular disease and cancer. *Am. J. Med.* 2002, *113*, 71–88.

(5) Robak, J.; Gryglewski, R. J. Bioactivity of flavonoids. *Pol. J. Pharmacol.* 1996, *48*, 555–564.

(6) Rice-Evans, C. A.; Spencer, J. P.; Schroeter, H.; Rechner, A. R. Bioavailability of flavonoids and potential bioactive forms *in vivo*. *Drug Metab. Drug Interact.* 2000, *17*, 291–310.

(7) Clifford, M. N. Chlorogenic acids and other cinnamates − nature, occurence and dietary burden. *J. Sci. Food Agric.* 1999, *79*, 362–372.

(8) Rencher, A. R.; Spencer, P. E.; Kuhnle, G.; Hahn, U.; Rice-Evans, C. A. Novel biomarkers of the metabolism of caffeic acid derivatives *in vivo*. *Free Radical Biol. Med.* 2001, *30*, 1213–1222.

(9) Hermann, K. Flavonoid antioxidants in food of plant origin. *Gordian* 1993, No. 7−8, 108–111.

(10) Renaud, S.; De Lorgeril, M. Wine, alcohol, platelets, and the French paradox for coronary heart disease. *Lancet* 1992, *339*, 1523–1526.

(11) Frankel, E. N.; Kanner, J.; German, J. B.; Parks, E.; Kinsella, J. E. Inhibition of oxidation of human low-density lipoprotein by phenolic substances in red wine. *Lancet* 1993, *341*, 454–457.

(12) Hertog, M. G. L.; Freskens, E. J. M.; Hollman, P. C. H.; Katan, M. B.; Kromhout, D. Dietary antioxidative flavonoids and risk of coronary heart disease: the Zutphen Elderly Study. *Lancet* 1993, *342*, 1007–1011.

(13) Robbins, R. J. Phenolic acids in foods: an overview of analytical methodology. *J. Agric. Food Chem.* 2003, *51*, 2866–2887.

(14) King, A.; Young, G. Characteristics and occurrence of phenolic phytochemicals. *J. Am. Diet. Assoc.* 1999, *99*, 213–218.

(15) Strack, D.; Wray, V. Anthocyanins. In *Methods in Plant Biochemistry, Plant Phenolics*; Harborne, J. B., Ed.; Academic Press: London, U.K., 1993; Vol. 1, pp 325−356.

(16) Stinzing, F. C.; Carle, R. Functional properties of anthocyanins and betalins in plants, food, and in human nutrition. *Trends Food Sci. Technol.* 2004, *15*, 19–38.

(17) Zhang, Y.; Vareed, S. K.; Nair, M. G. Human tumor cell growth inhibition by nontoxic anthocyanidins, the pigments in fruits and vegetables. *Life Sci.* 2005, *76*, 1465–1472.

(18) Jayaprakasam, B.; Vareed, S. K.; Olson, L. K.; Nair, M. G. Insulin secretion by bioactive anthocyanins and anthocyanidins present in fruits. *J. Agric. Food Chem.* 2005, *53*, 28–31.

(19) Matsui, T.; Ueda, T.; Oki, T.; Sugita, K.; Terahara, N.; Matsumoto, K. α-Glucosidase inhibitory action of natural acylated anthocyanins. 1. Survey of natural pigments with potent inhibitory activity. *J. Agric. Food Chem.* 2001, *49*, 1948–1951.

(20) Tall, J. M.; Seeram, N. P.; Zhao, C. S.; Nair, M. G.; Meyer, R. A.; Raja, S. N. Tart cherry anthocyanins suppress inflammation-induced pain behavior in rat. *Behav. Brain Res.* 2004, *153*, 181–192.

(21) Revilla, I.; González-SanJosé, M. L. Effect of different oak woods on aged wine color and anthocyanin composition. *Eur. Food Res. Technol.* 2001, *213*, 281–285.

(22) Brouillard, R.; Chassaing, S.; Fougerousse, A. Why are grape/fresh wine anthocyanins so simple and why is it that red wine color lasts so long? *Phytochemistry* 2003, *64*, 1179–1186.

(23) Somers, T. C. The polymeric nature of wine pigments. *Phytochemistry* 1971, *10*, 2175–2186.

(24) Jurd, L. Review of polyphenol condensation reactions and their possible occurrence in the aging of wines. *Am. J. Enol. Vitic.* 1969, *20*, 191–195.

(25) Liao, H.; Cai, Y.; Haslam, E. Polyphenol interactions. Anthocyanins: copigmentation and colour changes in red wines. *J. Sci. Food Agric.* 1992, *59*, 299–305.

(26) Remy, S.; Fulcrand, H.; Labarbe, B.; Cheynier, V.; Moutounet, M. First confirmation in red wine of products resulting from direct anthocyanin-tannin reactions. *J. Sci. Food Agric.* 2000, *80*, 745–751.

(27) Bakker, J.; Picinelli, A.; Bridle, P. Model wine solutions: colour and composition changes during ageing. *Vitis* 1993, *32*, 111–118.

(28) Rivas-Gonzalo, J. C.; Bravo-Haro, S.; Santos-Buelga, C. Detection of compounds formed through the reaction of malvidin-3-monoglucoside and catechin in the presence of acetaldehyde. *J. Agric. Food Chem.* 1995, *43*, 1444–1449.

(29) Timberlake, C. F.; Bridle, P. Interactions between anthocyanins, phenolics compounds and acetaldehyde, and their significance in red wines. *Am. J. Enol. Vitic.* 1976, *27*, 97–105.

(30) Bakker, J.; Bridle, P.; Honda, T.; Kuwano, H.; Saito, N.; Terahara, N.; Timberlake, C. F. Identification of an anthocyanin occurring in some red wines. *Phytochemistry* 1997, *44*, 1375–1382.

(31) Bakker, J.; Timberlake, C. F. Isolation, identification, and characterization of new color-stable anthocyanins occurring in some red wines. *J. Agric. Food Chem.* 1997, *45*, 35–43.

(32) Fulcrand, H.; Benabdeljalil, C.; Rigaud, J.; Cheynier, V.; Moutounet, M. A new class of wine pigments generated by reaction between pyruvic acid and grape anthocyanins. *Phytochemistry* 1998, *47*, 1401–1407.

(33) Romero, C.; Bakker, J. Interactions between grape anthocyanins and pyruvic acid, with effect of pH and acid concentration on anthocyanin composition and color in model solutions. *J. Agric. Food Chem.* 1999, *47*, 3130–3139.

(34) Mateus, N.; Silva, A. M. S.; Vercauteren, J.; De Freitas, V. Occurrence of anthocyanin-derived pigments in red wines. *J. Agric. Food Chem.* 2001, *49*, 4836–4840.

(35) Mateus, N.; De Freitas, V. Evolution and stability of anthocyanin-derived pigments during Port wine aging. *J. Agric. Food Chem.* 2001, *49*, 5217–5222.

(36) Cameira dos Santos, P. J.; Brillouet, J. M.; Cheynier, V.; Moutounet, M. Detection and partial characterisation of new anthocyanin-derived pigments in wine. *J. Sci. Food Agric.* 1996, *70*, 204–208.

(37) Fulcrand, H.; Cameira dos Santos, P. J.; Sarni-Manchado, P; Cheynier, V.; Favre-Bonvin, J. Structure of new anthocyanin-derived wine pigments. *J. Chem. Soc., Perkin Trans. 1* 1996, 735–739.

(38) Schwarz, M.; Wabnitz, T. C.; Winterhalter, P. Pathway leading to the formation of anthocyaninvinylphenol adducts and related pigments in red wines. *J. Agric. Food Chem.* 2003, *51*, 3682–3687.

(39) Benabdeljalil, C.; Cheynier, V.; Fulcrand, H.; Hakiki, A.; Mosaddak, M.; Moutounet, M. Mise en evidence de nouveaux pigments formes par reaction des anthocyanes avec des metabolites de levures. *Sci. Aliments.* 2000, *20*, 203–220.

(40) Lu, Y.; Foo, L. Y. Unusual anthocyanin reaction with acetone leading to pyranoanthocyanin formation. *Tetrahedron Lett.* 2001, *42*, 1371–1373.

(41) Hayasaka, Y.; Asenstorfer, R. E. Screening for potential pigments derived from anthocyanins in red wine using nanoelectrospray tandem mass spectrometry. *J. Agric. Food Chem.* 2002, *50*, 756–761.

(42) Wright, J. S.; Johnson, E. R.; Di Labio, G. A. Predicting the activity of phenolic antioxidants: theoretical method, analysis of substituent effects and application to major families of antioxidants. *J. Am. Chem. Soc.* 2001, *123*, 1173–1183.

(43) Leopoldini, M.; Prieto Pitarch, I.; Russo, N.; Toscano, M. Structure, conformation and electronic properties of apigenin, luteolin and taxifolin antioxidants. A first principle theoretical study. *J. Phys. Chem. B* 2004, *108*, 92–94.

(44) Leopoldini, M.; Marino, T.; Russo, N.; Toscano, M. Antioxidant properties of phenolic compounds. H-atom versus electron transfer mechanism. *J. Phys. Chem. B* 2004, *108*, 4916–4922.

(45) Leopoldini, M.; Marino, T.; Russo, N.; Toscano, M. Density functional computations of the energetic and spectroscopic parameters

of quercetin and its radicals in the gas phase and in solvent. *Theor. Chem. Acc*. **2004**, *111*, 210–216.

(46) Leopoldini, M.; Russo, N.; Chiodo, S.; Toscano, M. Iron chelation by the powerful antioxidant flavonoid quercetin. *J. Agric. Food Chem.* **2006**, *54*, 6343–6351.

(47) Cornard, J. P.; Dangleterre, L.; Lapouge, C. Computational ands characterization of the molecular and electronic structure of the Pb(II)−quercetin complex. *J. Phys. Chem. A* **2005**, *109*, 10044–10051.

(48) Cornard, J. P.; Merlin, J. C. Spectroscopic and structural study of complexes of quercetin with Al(III). *J. Inorg. Biochem*. **2002**, *92*, 19–27.

(49) Fiorucci, S.; Golebiowski, J.; Cabrol-Bass, D.; Antonczak, S. DFT study of quercetin activated forms involved in antiradical, antioxidant, and prooxidant biological processes. *J. Agric. Food Chem.* **2007**, *55*, 903–911.

(50) Frisch, M. J.; Trucks, G. W.; Schlegel, H. B.; Scuseria, G. E.; Robb, M. A.; Cheeseman, J. R.; Montgomery, J. A., Jr.; Vreven, T.; Kudin, K. N.; Burant, J. C.; Millam, J. M.; Iyengar, S. S.; Tomasi, J.; Barone, V.; Mennucci, B.; Cossi, M.; Scalmani, G.; Rega, N.; Petersson, G. A.; Nakatsuji, H.; Hada, M.; Ehara, M.; Toyota, K.; Fukuda, R.; Hasegawa, J.; Ishida, M.; Nakajima, T.; Honda, Y.; Kitao, O.; Nakai, H.; Klene, M.; Li, X.; Knox, J. E.; Hratchian, H. P.; Cross, J. B.; Adamo, C.; Jaramillo, J.; Gomperts, R.; Stratmann, R. E.; Yazyev, O.; Austin, A. J.; Cammi, R.; Pomelli, C.; Ochterski, J. W.; Ayala, P. Y.; Morokuma, K.; Voth, G. A.; Salvador, P.; Dannenberg, J. J.; Zakrzewski, V. G.; Dapprich, S.; Daniels, A. D.; Strain, M. C.; Farkas, O.; Malick, D. K.; Rabuck, A. D.; Raghavachari, K.; Foresman, J. B.; Ortiz, J. V.; Cui, Q.; Baboul, A. G.; Clifford, S.; Cioslowski, J.; Stefanov, B. B.; Liu, G.; Liashenko, A.; Piskorz, P.; Komaromi, I.; Martin, R. L.; Fox, D. J.; Keith, T.; Al-Laham, M. A.; Peng, C. Y.; Nanayakkara, A.; Challacombe, M.; Gill, P. M. W.; Johnson, B.; Chen, W.; Wong, M. W.; Gonzalez, C.; Pople, J. A. *Gaussian03*; Gaussian, Inc.: Pittsburgh, PA, 2003.

(51) Woodford, J. A DFT investigation of anthocyanidins. *Chem. Phys. Lett.* **2005**, *410*, 182–187.

(52) Carvalho, A. R. F.; Oliveira, J.; De Freitas, V.; Silva, A.; Mateus, N.; Melo, A. A computational study of vinylpyranoanthocyanin-phenolic pigments (portisins). *J. Mol. Struct.* (*THEOCHEM*) **2009**, *xxx*, xxx–xxx.

(53) Freitas, A. A.; Shimizu, K.; Dias, L. G.; Quina, F. H. A computational study of substituted flavylium salts and their quinonoidal conjugate-bases: $S_0{\rightarrow}S_1$ electronic transition, absolute pK_a and reduction potential calculations by DFT and semiempirical methods. *J. Braz. Chem. Soc* **2007**, *18*, 1537–1546.

(54) Sakata, K.; Saito, N.; Honda, T. Ab initio study of molecular structures and excited states in anthocyanins. *Tetrahedron* **2006**, *62*, 372–3731.

(55) Guzmán, R.; Santiago, C.; Sánchez, M. A density functional study of antioxidant properties on anthocyanidins. *J. Mol. Struct.* (*THEOCHEM*) **2009**, *935*, 110–114.

(56) Estevez, L.; Mosquera, R. A. Conformational and substitution effects on the electron distribution in a series of anthocyanidins. *J. Phys. Chem. A* **2009**, *113*, 9908–9919.

(57) Borkowski, T.; Szymusiak, H.; Gliszczynska-Swigło, A.; Rietjens, I. M. C. M.; Tyrakowska, B. Radical scavenging capacity of wine anthocyanins is strongly pH-dependent. *J. Agric. Food Chem.* **2005**, *53*, 5526–5534.

(58) Estevez, L.; Mosquera, R. A. Molecular structure and antioxidant properties of delphinidin. *J. Phys. Chem. A* **2008**, *112*, 10614–10623.